

SHAPE MEMORY MATERIALS

Edited by

K. OTSUKA

Institute of Materials Science, University of Tsukuba

and

C. M. WAYMAN

*Department of Materials Science and Engineering,
University of Illinois*



CAMBRIDGE
UNIVERSITY PRESS

PUBLISHED BY THE PRESS SYNDICATE OF THE UNIVERSITY OF CAMBRIDGE
The Pitt Building, Trumpington Street, Cambridge, United Kingdom

CAMBRIDGE UNIVERSITY PRESS
The Edinburgh Building, Cambridge CB2 2RU, UK www.cup.cam.ac.uk
40 West 20th Street, New York, NY 10011-4211, USA www.cup.org
10 Stamford Road, Oakleigh, Melbourne 3166, Australia
Ruiz de Alarcón 13, 28014, Madrid, Spain

© Cambridge University Press 1998

This book is in copyright. Subject to statutory exception
and to the provisions of relevant collective licensing agreements,
no reproduction of any part may take place without
the written permission of Cambridge University Press.

First published 1998
First paperback edition (with corrections) 1999

Typeset in 11/14 pt Times New Roman [vN]

A catalogue record for this book is available from the British Library

Library of Congress Cataloguing in Publication data

Shape memory materials / edited by K. Otsuka and C. M. Wayman

p. cm.

ISBN 0 521 44487 X (hc)

1. Shape memory alloys. I. Otsuka, Kazuhiro, 1937–

II. Wayman, Clarence Marvin, 1930–

TA487.548 1998

620.1'632–dc21 97–38119 CIP

ISBN 0 521 44487 X hardback

ISBN 0 521 663849 paperback

Transferred to digital printing 2002

Contents

<i>List of contributors</i>	page xi
<i>Preface</i>	xiii
1 Introduction	1
<i>K. Otsuka and C. M. Wayman</i>	
1.1 Invitation to shape memory effect and the notion of martensitic transformation	1
1.2 Martensitic transformations: crystallography	5
1.3 Martensitic transformations: thermodynamic aspects	21
2 Mechanism of shape memory effect and superelasticity	27
<i>K. Otsuka and C. M. Wayman</i>	
2.1 Stress-induced martensitic transformation and superelasticity	27
2.2 Shape memory effect	36
2.3 Rubber-like behavior	44
3 Ti–Ni shape memory alloys	49
<i>T. Saburi</i>	
3.1 Structure and transformations	49
3.2 Mechanical behavior of Ti–Ni alloys	58
3.3 Ternary alloying	73
3.4 Self-accommodation in martensites	79
3.5 All-round shape memory (Two-way shape memory)	84
3.6 Effects of irradiation on the shape memory behavior	87
3.7 Sputter-deposited films of Ti–Ni alloys	87
3.8 Melt-spun ribbons of Ti–Ni alloys	93
4 Cu-based shape memory alloys	97
<i>T. Tadaki</i>	
4.1 Phase diagrams of typical Cu-based shape memory alloys	97
4.2 Mechanical behavior	100

4.3	Aging effects of shape memory alloys	105
4.4	Thermal cycling effects	109
4.5	Improvements of shape memory alloys	112
5	Ferrous shape memory alloys	117
	<i>T. Maki</i>	
5.1	Morphology and substructure of ferrous martensite	117
5.2	Ferrous alloys exhibiting shape memory effect	118
5.3	Shape memory effect associated with α' thin plate martensite	121
5.4	Shape memory effect associated with ε martensite in Fe–Mn–Si alloys	126
6	Fabrication of shape memory alloys	133
	<i>Y. Suzuki</i>	
6.1	Fabrication of Ti–Ni based alloys	134
6.2	Fabrication of Cu–Al–Zn based alloys	143
6.3	Powder metallurgy and miscellaneous methods	145
7	Characteristics of shape memory alloys	149
	<i>J. Van Humbeeck and R. Stalmans</i>	
7.1	Summary of the functional properties	149
7.2	A generalized thermodynamic description of shape memory behaviour	151
7.3	Two-way memory behaviour	159
7.4	Constrained recovery – generation of recovery stresses	162
7.5	The high damping capacity of shape memory alloys	165
7.6	Cycling effects, fatigue and degradation of shape memory alloys	168
7.7	Property values	178
8	Shape memory ceramics	184
	<i>K. Uchino</i>	
8.1	Development trends of new principle actuators	184
8.2	Shape memory ceramics	185
8.3	Sample preparation and experiments	189
8.4	Fundamental properties of the electric field-induced phase transition	190
8.5	Comparison with shape memory alloys	198
8.6	Applications of shape memory ceramics	199
8.7	Conclusions	202
9	Shape memory polymers	203
	<i>M. Irie</i>	
9.1	Shape memory effect of polymer materials	203

9.2	Thermal-responsive shape memory effect	206
9.3	Photo-responsive shape memory effect	212
9.4	Chemo-responsive shape memory effect	218
10	General applications of SMA's and smart materials	220
	<i>K. N. Melton</i>	
10.1	Introduction	220
10.2	History of applications of SMA	221
10.3	SMA couplings	222
10.4	Electrical connectors	226
10.5	Fastener type applications	230
10.6	History of applications of superelasticity	232
10.7	Selection criteria for SMA applications	234
10.8	Smart materials	237
11	The design of shape memory alloy actuators and their applications	240
	<i>I. Ohkata and Y. Suzuki</i>	
11.1	Characteristics of shape memory alloy actuators	240
11.2	The design of shape memory alloy springs	242
11.3	The design of two-way actuators	247
11.4	Shape memory alloy actuator applications	254
12	Medical and dental applications of shape memory alloys	267
	<i>S. Miyazaki</i>	
12.1	Introduction	267
12.2	Application examples	267
12.3	Corrosion resistance	276
12.4	Elution test	278
12.5	Biocompatibility	279
	<i>Index</i>	282

1

Introduction

K. OTSUKA AND C. M. WAYMAN

Symbols for Chapters 1 and 2

A_f reverse transformation finish temperature	M_f martensite finish temperature
A_s reverse transformation start temperature	M_s martensite start temperature
B lattice deformation matrix	p hydrostatic pressure
d_1 shape strain direction (unit column vector)	p_1' invariant plane normal (habit plane normal) (p_1' unit row vector)
F_d diagonal matrix	P_1 shape strain matrix
F_s symmetric matrix	P_2 lattice invariant shear matrix
g^m chemical free energy of the martensitic phase per unit volume	R rhombohedral (Ramsdel notation)
g^p chemical free energy of the parent phase per unit volume	R rotation matrix
$\Delta g_c = g^m - g^p$ chemical free energy change upon martensitic transformation per unit volume	s twinning shear
G^m Gibbs free energy of the martensitic phase	ΔS entropy of transformation
G^p Gibbs free energy of the parent phase	T temperature
$\Delta G^{p-m} = G^m - G^p$	T_0 equilibrium temperature between parent and martensite
ΔG^s free energy change due to an applied stress	V volume of the parent phase
$\Delta G_c = \Delta G^{p-m}$ chemical free energy change upon martensitic transformation	ΔV volume change upon martensitic transformation
ΔG_c strain energy arising from martensitic transformation	ε strain associated with the martensitic transformation
$\Delta G_{nc} = \Delta G_s + \Delta G_c$ non-chemical term in the free energy change upon martensitic transformation	ε_c calculated transformation strain
ΔG_s surface energy arising from martensitic transformation	η_1 twinning shear direction
H hexagonal (Ramsdel notation)	η_2 the intersection of the plane of shear and the K_2 plane
ΔH^* enthalpy of transformation	λ an angle between the shear component of the shape strain and the tensile axis
I identity matrix	σ applied stress
K_1 twinning plane	σ_n normal component of an applied stress along the habit plane normal
K_2 undistorted plane	τ shear stress component of an applied stress along the shear component of the shape strain
m_1 magnitude of shape strain	χ an angle between the habit plane and the tensile axis
m_1^d dilatational component of shape strain ($\Delta V/V$)	
m_1^p shear component of shape strain	

1.1 Invitation to shape memory effect and the notion of martensitic transformation

The shape memory effect (to be abbreviated SME hereafter) is a unique property of certain alloys exhibiting martensitic transformations, as typically

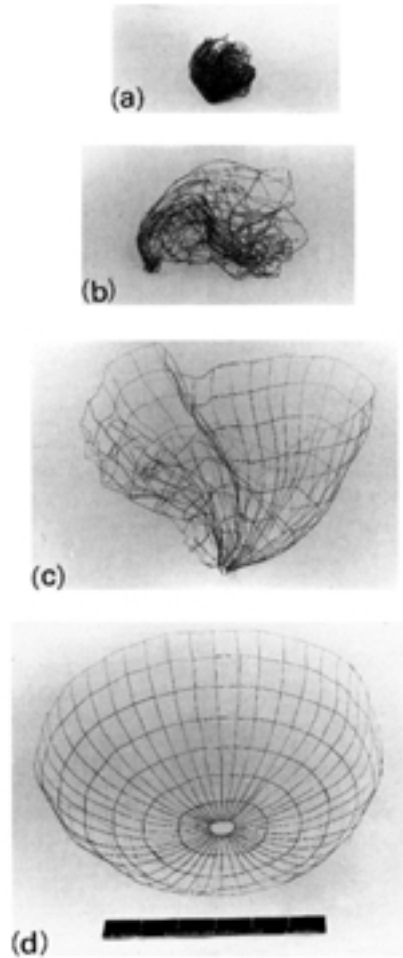


Fig. 1.1. Demonstration of shape memory effect by a space antenna of Ti-Ni wires. The antenna deformed in the martensitic state in (a) reverts to the original shape (b-d) upon heating by solar heat. (Courtesy Goodyear Aerospace Corporation)

shown in Fig. 1.1. Even though the alloy is deformed in the low temperature phase, it recovers its original shape by the reverse transformation upon heating to a critical temperature called the reverse transformation temperature. This effect was first found in a Au-47.5 at% Cd alloy by Chang and Read,¹ and then it was publicized with the discovery in Ti-Ni alloys by Buehler *et al.*² Many other alloys such as In-Tl,^{3,4} Cu-Zn⁵ and Cu-Al-Ni⁶ were found between the above two and thereafter. (See Ref. [7] for historical developments.) The same alloys have another unique property called ‘superelasticity’ (SE) at a higher temperature, which is associated with a large (several–18%) nonlinear recoverable strain upon loading and unloading. Since these alloys have a unique

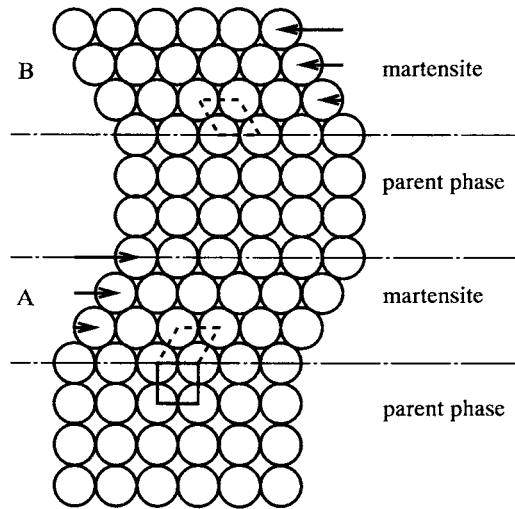


Fig. 1.2. A simplified model of martensitic transformation. See text for details.

property in remembering the original shape, having an actuator function and having superelasticity, they are now being used for various applications such as pipe couplings, various actuators in electric appliances, automobile applications, antennae for cellular phones and medical implants and guidewires etc. Besides, since they have the function of an actuator as well as a sensor, they are promising candidates for miniaturization of actuators such as microactuators or micromachines or robots. These will be discussed in detail in later chapters.

Since both SME and SE are closely related to the martensitic transformation (MT), the basic notion of MT is first given in a very naive and oversimplified manner. More accurate descriptions will follow in the next section. The martensitic transformation is a diffusionless phase transformation in solids, in which atoms move cooperatively, and often by a shear-like mechanism. Usually the parent phase (a high temperature phase) is cubic, and the martensite (a lower temperature phase) has a lower symmetry. The transformation is schematically shown in Fig. 1.2. When the temperature is lowered below some critical one, MT starts by a shear-like mechanism, as shown in the figure. The martensites in region A and in region B have the same structure, but the orientations are different. These are called the correspondence variants of the martensites. Since the martensite has a lower symmetry, many variants can be formed from the same parent phase. Now, if the temperature is raised and the martensite becomes unstable, the reverse transformation (RT) occurs, and if it is crystallographically reversible, the martensite reverts to the parent phase in the original orientation. This is the origin of SME, which will be described in

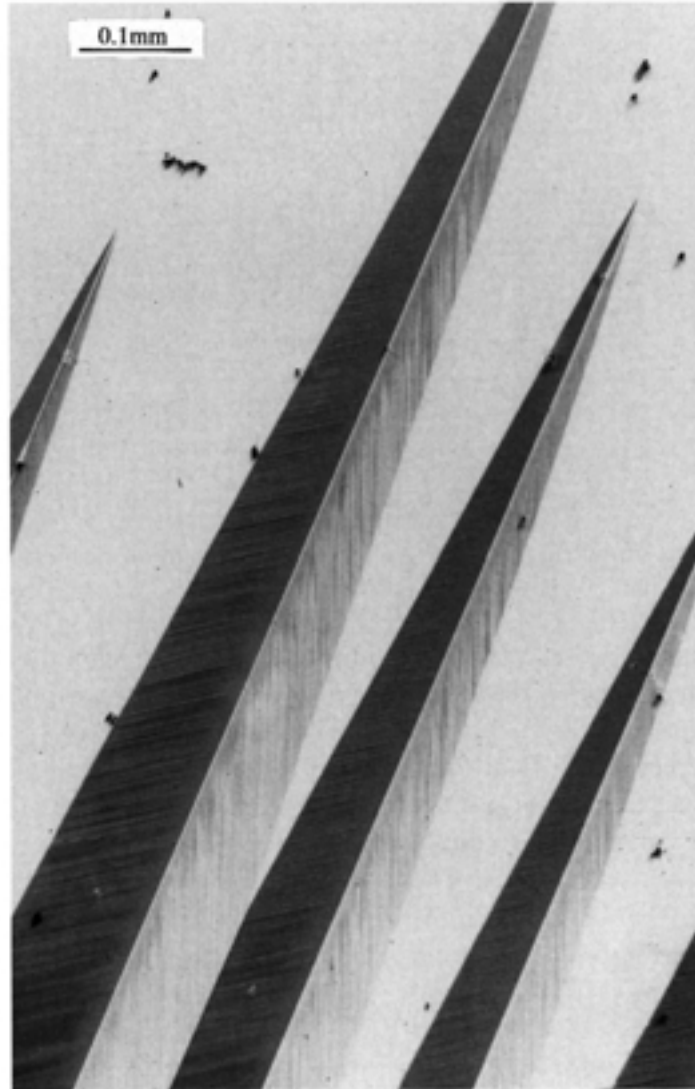


Fig. 1.3. Optical micrograph of spear-like γ_1' martensite in Cu–14.2 mass% Al–4.2 mass% Ni alloy.

more detail later. The above example clearly shows that the characteristics of MT lie in the cooperative movement of atoms. Because of this nature, MT is sometimes called the displacive transformation or military transformation, which are equivalent in usage to MT. Thus, even though the relative atomic displacements are small (compared with inter-atomic distance), a macroscopic shape change appears associated with MT, as seen in Fig. 1.2. It is in this respect that MT is closely related to SME and SE.

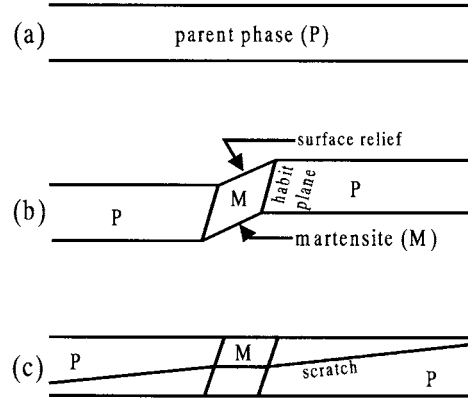


Fig. 1.4. Schematic representation of shape change associated with martensitic transformation; (a) original parent single crystal, (b) surface relief due to transformation, (c) change in direction of pre-scratched straight line upon martensitic transformation.

Figure 1.3 shows an optical micrograph of a typical martensite in a Cu–Al–Ni alloy. The flat region in light contrast represents a parent phase, while the plate-like morphology of martensite variants is observable by surface relief (surface upheaval) effects. The thin band contrasts in each martensite variant are twins, which will be discussed later. Similarly, when a straight line is marked on the surface of a specimen, the line changes direction upon MT, as schematically shown in Fig. 1.4(c). These experiments clearly show that the shape change associated with MT is linear, since upon MT, a line and a surface are changed into another line and surface, respectively. This means that the shape change associated with MT can be described by a matrix *as an operator*.

1.2 Martensitic transformations: crystallography

1.2.1 Linear algebra describing a deformation (mathematical preparation)

When a deformation is linear, the deformation is represented by the following equation.

$$\begin{pmatrix} x_2 \\ y_2 \\ z_2 \end{pmatrix} = \begin{pmatrix} a_{11} & a_{12} & a_{13} \\ a_{21} & a_{22} & a_{23} \\ a_{31} & a_{32} & a_{33} \end{pmatrix} \begin{pmatrix} x_1 \\ y_1 \\ z_1 \end{pmatrix}. \quad (1.1)$$

In a compact form, it may be written as

$$\mathbf{r}_2 = \mathbf{A}\mathbf{r}_1, \quad (1.2)$$

where \mathbf{A} represents the matrix a_{ij} etc. That is, any vector \mathbf{r}_1 is transformed into

r_2 by a matrix A as an operator. The examples of A will be given in the following sections. When we use linear algebra, a coordinate transformation is also necessary, since we refer to both the parent phase and the martensite, which have different structures. There are some important formulas for a coordinate transformation, which apply for any crystal system. Suppose we have two axis systems represented by the base vectors $\mathbf{a}, \mathbf{b}, \mathbf{c}$ (we call this the old system) and $\mathbf{A}, \mathbf{B}, \mathbf{C}$ (we call this the new system). Then, we can immediately write down Eq. (1.3). Then, by solving $\mathbf{a}, \mathbf{b}, \mathbf{c}$ as a function of $\mathbf{A}, \mathbf{B}, \mathbf{C}$ in Eq. (1.3), we obtain Eq. (1.4). These equations represent the relations between the old and the new axis systems in direct space. However, it is proven that similar equations hold in reciprocal space as shown in Eqs. (1.5) and (1.6), where $\mathbf{a}^*, \mathbf{b}^*, \mathbf{c}^*$ represent the base vectors in reciprocal space, which correspond to $\mathbf{a}, \mathbf{b}, \mathbf{c}$, and the same thing applies to $\mathbf{A}^*, \mathbf{B}^*, \mathbf{C}^*$.⁸

$$\begin{aligned} \mathbf{A} &= s_{11}\mathbf{a} + s_{12}\mathbf{b} + s_{13}\mathbf{c} \\ \mathbf{B} &= s_{21}\mathbf{a} + s_{22}\mathbf{b} + s_{23}\mathbf{c} \\ \mathbf{C} &= s_{31}\mathbf{a} + s_{32}\mathbf{b} + s_{33}\mathbf{c} \end{aligned} \quad (1.3)$$

$$\begin{aligned} \mathbf{a} &= t_{11}\mathbf{A} + t_{12}\mathbf{B} + t_{13}\mathbf{C} \\ \mathbf{b} &= t_{21}\mathbf{A} + t_{22}\mathbf{B} + t_{23}\mathbf{C} \\ \mathbf{c} &= t_{31}\mathbf{A} + t_{32}\mathbf{B} + t_{33}\mathbf{C} \end{aligned} \quad (1.4)$$

$$\begin{aligned} \mathbf{A}^* &= t_{11}\mathbf{a}^* + t_{21}\mathbf{b}^* + t_{31}\mathbf{c}^* \\ \mathbf{B}^* &= t_{12}\mathbf{a}^* + t_{22}\mathbf{b}^* + t_{32}\mathbf{c}^* \\ \mathbf{C}^* &= t_{13}\mathbf{a}^* + t_{23}\mathbf{b}^* + t_{33}\mathbf{c}^* \end{aligned} \quad (1.5)$$

$$\begin{aligned} \mathbf{a}^* &= s_{11}\mathbf{A}^* + s_{21}\mathbf{B}^* + s_{31}\mathbf{C}^* \\ \mathbf{b}^* &= s_{12}\mathbf{A}^* + s_{22}\mathbf{B}^* + s_{32}\mathbf{C}^* \\ \mathbf{c}^* &= s_{13}\mathbf{A}^* + s_{23}\mathbf{B}^* + s_{33}\mathbf{C}^* \end{aligned} \quad (1.6)$$

Furthermore, there are other important formulas for arbitrary vector components in direct and in reciprocal space, as shown below.

$$\begin{pmatrix} x \\ y \\ z \end{pmatrix} = \begin{pmatrix} s_{11} & s_{21} & s_{31} \\ s_{12} & s_{22} & s_{32} \\ s_{13} & s_{23} & s_{33} \end{pmatrix} \begin{pmatrix} X \\ Y \\ Z \end{pmatrix} \quad (1.7)$$

old \mathbf{A} \mathbf{B} \mathbf{C} new

$$\begin{pmatrix} H \\ K \\ L \end{pmatrix} = \begin{pmatrix} s_{11} & s_{12} & s_{13} \\ s_{21} & s_{22} & s_{23} \\ s_{31} & s_{32} & s_{33} \end{pmatrix} \begin{pmatrix} h \\ k \\ l \end{pmatrix} \quad (1.8)$$

new old

where xyz and XYZ refer to the direct lattice (i.e. direction) and hkl and HKL to the reciprocal lattice (i.e. plane).

When a coordinate transformation is applied for a vector or a plane, an operator is also transformed following the similarity transformation given below. (The proof is simple. See Ref. [9] for the proof.)

$$\bar{A} = R^{-1}AR \text{ or } A = R\bar{A}R^{-1} \quad (1.9)$$

$$\bar{A} = R^TAR \text{ or } A = R\bar{A}R^T \text{ (when } R \text{ is orthogonal),} \quad (1.10)$$

where A is an operator in the old system, while \bar{A} is that in the new system, R is a rotation matrix, and R^{-1} is an inverse of R , and R^T is R transposed. In the martensite crystallography calculations, the similarity transformation is often used, since operators often refer to the parent phase in such calculations.

1.2.2 Structural change without diffusion: lattice correspondence, correspondence variant and lattice deformation

We now discuss how the martensite crystal is produced from the parent crystal without diffusion. As a typical example, we describe this for the well-known FCC (Face-Centered Cubic)–BCT (Body-Centered Tetragonal) transformation in steels. Figure 1.5(a) shows two FCC unit cells, in which we notice a BCT lattice with the axial ratio $c/a = \sqrt{2}$. Thus, if the X and Y axes in the figure are elongated and the Z axis is contracted so that c/a becomes the value of the martensite (i.e. a value close to 1), then a BCT martensite is created, as shown in Fig. 1.5(b). This is the mechanism originally proposed by Bain.¹⁰ Although the mechanism is different from one alloy to another, it is always possible to create a martensite from a parent by the combination of elongation, contraction and shear along certain directions. If the lattice parameter of the FCC is a_0 , and those of the BCT are a and c , then the lattice deformation matrix with respect to the XYZ axes is written as follows.

$$\mathbf{B} = \begin{pmatrix} \sqrt{2}a/a_0 & 0 & 0 \\ 0 & \sqrt{2}a/a_0 & 0 \\ 0 & 0 & c/a_0 \end{pmatrix} \quad (1.11)$$

By utilizing the similarity transformation, the lattice deformation matrix with

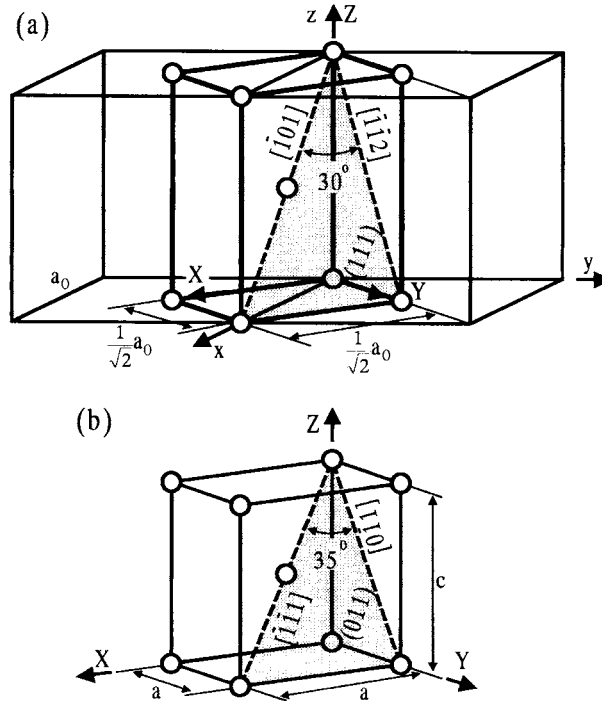


Fig. 1.5. Mechanism of FCC–BCT (or BCC) transformation by Bain. xyz represents the crystal axes in the parent FCC lattice, while XYZ represents those axes in the BCT martensite. See text for details.

respect to the parent lattice (i.e. the xyz axes in (a)) is given as follows.

$$\begin{aligned}
 \mathbf{B} &= \mathbf{R}\bar{\mathbf{B}}\mathbf{R}^T \\
 &= \begin{pmatrix} 1/\sqrt{2} & 1/\sqrt{2} & 0 \\ -1/\sqrt{2} & 1/\sqrt{2} & 0 \\ 0 & 0 & 1 \end{pmatrix} \begin{pmatrix} \sqrt{2}a/a_0 & 0 & 0 \\ 0 & \sqrt{2}a/a_0 & 0 \\ 0 & 0 & c/a_0 \end{pmatrix} \begin{pmatrix} 1/\sqrt{2} & -1/\sqrt{2} & 0 \\ 1/\sqrt{2} & 1/\sqrt{2} & 0 \\ 0 & 0 & 1 \end{pmatrix}. \quad (1.12)
 \end{aligned}$$

Another important notion is the lattice correspondence, which is associated with the lattice deformation. Since MT is diffusionless, there is a one-to-one correspondence in the directions and planes between the parent and the martensite. It is clear in the figure that $[1/2 \ 1/2 \ 0]_p$ and $[1/2 \ 1/2 \ 0]_p$ correspond to $[100]_m$ and $[010]_m$, respectively, where the subscripts p and m correspond to parent and martensite respectively. Then, how an arbitrary $[xyz]_p$ and $(hkl)_p$ in the parent phase correspond to which $[XYZ]_m$ and $(HKL)_m$ in the martensite is the main problem here. This is essentially the problem of coordinate

transformation. In Fig. 1.5(a), it is easy to write down the coordinate transformation between the xyz system and the XYZ system. When we transform from the XYZ system in (a) to the $X'Y'Z'$ system in (b), lattice change (by lattice deformation) occurs, but the Miller indices are invariant under this transformation. Thus, the above obtained equation of coordinate transformation still holds, as follows.

$$\begin{array}{ccc} \begin{pmatrix} x \\ y \\ z \end{pmatrix} = \begin{pmatrix} 1/2 & 1/2 & 0 \\ -1/2 & 1/2 & 0 \\ 0 & 0 & 1 \end{pmatrix} \begin{pmatrix} X \\ Y \\ Z \end{pmatrix}, & \begin{pmatrix} H \\ K \\ L \end{pmatrix} = \begin{pmatrix} 1/2 & -1/2 & 0 \\ 1/2 & 1/2 & 0 \\ 0 & 0 & 1 \end{pmatrix} \begin{pmatrix} h \\ k \\ l \end{pmatrix}. & (1.13) \\ \text{old} & \text{new} & \text{new} & \text{old} \end{array}$$

From these equations, we can easily find that $[\bar{1}01]_p$ corresponds to $[\bar{1}\bar{1}1]_m$, $[\bar{1}\bar{1}2]_p$ to $[0\bar{1}1]_m$ and $(111)_p$ to $(011)_m$, by lattice correspondence.

One more important notion associated with lattice correspondence is the correspondence variant (c.v.). In Fig. 1.5, we chose the z axis as the c axis of the martensite. We could equally choose the x and y axes as the c axis of the martensite. Thus, three correspondence variants are possible in the FCC–BCT transformation.

Among many structural changes in various MTs, those in β -phase alloys are important. Thus, they are briefly described below. The β -phase alloys, such as Au–Cd, Ag–Cd, Cu–Al–(Ni), Cu–Zn–(Al) etc., are characterized by the value of electron/atom ratio $e/a \approx 1.5$, at which BCC (Body-Centered Cubic) or ordered BCC structure is stabilized due to nesting at the Brillouin zone boundary. The ordered BCC structures are usually B2 type or $D0_3$ type. With lowering temperature, these ordered BCC structures change martensitically into close-packed structures, which are called ‘long period stacking order structures’ with a two-dimensional close-packed plane (basal plane), since the entropy term in the Gibbs free energy becomes negligible at low temperatures and the decrease of internal energy becomes more important. Following Nishiyama and Kajiwara,¹¹ we describe the structural change for the B2 type parent phase using Fig. 1.6, but that for the $D0_3$ type parent phase is similar. The structure of the B2 type parent phase is shown in (a). This structure may be viewed as that in which the $(110)_{B2}$ plane is stacked in $A_1B_1A_1B_1 \dots$ order, as shown in (b). Upon MT, the $(110)_{B2}$ plane changes into a more close-packed plane $(001)_m$ in (c), by contracting along $[001]_{B2}$ and elongating along $[\bar{1}10]_{B2}$, so that the indicated angle changes from $70^\circ 32'$ to close to 60° . Once the plane becomes a close-packed one as shown in (c), we have three stacking positions A, B, C shown in (c). Then, we can create various stacking order structures. Theoretically, we can create an infinite number of long period stacking order

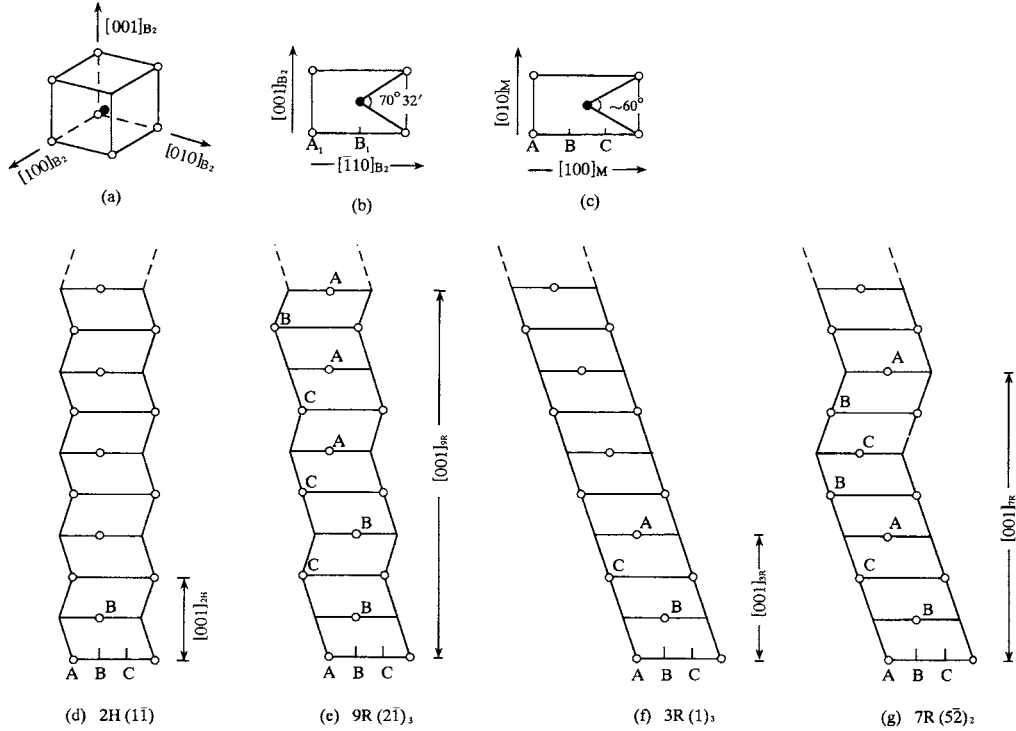


Fig. 1.6. The structural change from B2 parent phase into various martensites with long period stacking order structures. See text for details.

structures, but practically the first three (d–f) are most common, and the fourth (g) is a new one. There are two notations to describe these long period stacking order structures, i.e. Ramsdel notation and Zdanov symbol.^{12–14} The meanings of these notations are as follows. In (d), the period along the c -axis is 2, and the symmetry is hexagonal, when ordering is disregarded. Thus, it is called 2H in Ramsdel notation. The Zdanov symbols in parentheses represent the number of layers in a clockwise sequence (positive number) and that in an anti-clockwise sequence (negative number). Since the stacking sequence in the case of (d) is ABAB..., it is written as $(1\bar{1})$. In the case of (e), the period is 9, and the symmetry is rhombohedral. Thus, it is called 9R in Ramsdel notation. In the case of (g), 7R is the wrong notation, since it does not have rhombohedral symmetry, even though ordering is disregarded, but the term is commonly used erroneously. The usage of the two notations for (f) will be easily understood. In the above, the usage of Ramsdel notation is slightly different between Refs. [12,13] and Ref. [14]. We followed Refs. [12,13] by Kakinoki in the above. Thus care should be taken. There is another new notation proposed by the present authors¹⁵ which is more logical and more accurate. However, we

have omitted to describe it here, considering the character of this book and space limitation. For more details on MTs in β -phase alloys, see Refs. [16,17].

1.2.3 Lattice invariant shear and deformation twinning

Since MT is a first order transformation, it proceeds by nucleation and growth. Since MT is associated with a shape change as described above, a large strain arises around the martensite when it is formed in the parent phase. To reduce the strain is essentially important in the nucleation and growth processes of MT. There are two ways to attain it; either by introducing slip (b) or by introducing twins (c), as shown in Fig. 1.7(b) and (c). These are called the lattice invariant shear (LIS), since neither process changes the structure of the martensite. That is, either slip or twinning is a necessary process in MT for the above reason, and twins or dislocations are usually observed in martensites under electron microscopy. Which of slip or twinning is introduced depends upon the kind of alloys, but twinning is usually introduced as a LIS in SMAs. Thus, twinning is described in more detail in the following. Two twin crystals are generally related by a symmetry operation with respect to a mirror plane or a rotation axis. In deformation twinning, a twin is created by a proper shear, while twins are introduced upon MT for the above reason, and they can act as

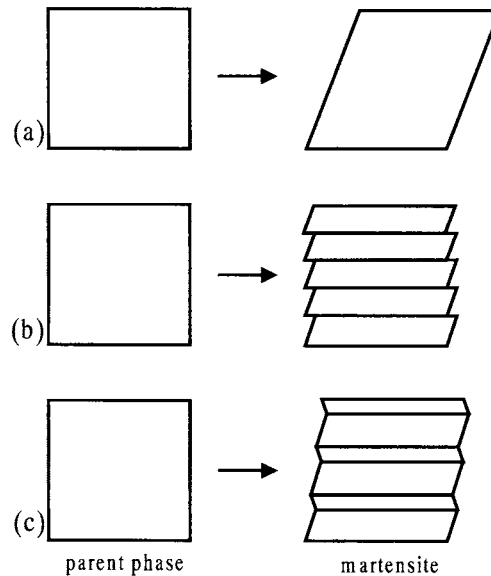


Fig. 1.7. Schematically shows why the lattice invariant shear is required upon martensitic transformation; (a) shape change upon martensitic transformation; (b) and (c) represent the accommodation of strain by introducing slip (b) or twins (c), respectively.

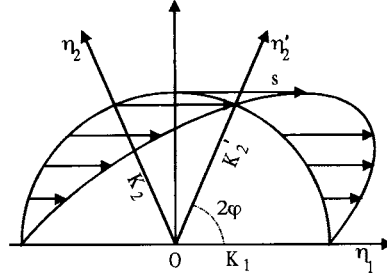


Fig. 1.8. The deformation of a unit sphere into an ellipsoid by shear, and the definition of K_1 , K_2 , η_1 , η_2 and s . See text for details.

a deformation mode under stress. In this connection twins have a close relationship with SME. Now, when we discuss deformation twinning, we use a unit sphere and an ellipsoid as a result of a shear, as shown in Fig. 1.8. In this shearing process, K_1 and η_1 represent the shear plane and the direction of the shear, respectively. Obviously K_1 is an invariant plane and K_2 is another undistorted plane in this process. The plane which is normal to K_1 and is parallel to η_1 is called the plane of shear, and the intersection of K_2 and the plane of shear is called η_2 . K_1 , K_2 , η_1 , η_2 and a twinning shear s are called the twinning elements. In order to create a twin by this process, the original lattice must be restored by this process. To satisfy the condition, there are two cases.¹⁸ In case I, two lattice vectors lie on the K_1 plane, and the third lattice vector is parallel to the η_2 direction. In this case, K_1 and η_2 are represented by rational indices, and the two twin crystals are related by a mirror symmetry with respect to the K_1 plane. This is called type I twinning. In case II, two lattice vectors lie on the K_2 plane, and the third lattice vector is parallel to the η_1 direction. In this case, K_2 and η_1 are represented by rational indices, K_1 and η_2 being irrational, and the two twin crystals are related by the rotation by π around the η_1 axis. This is called type II twinning. In some crystal systems, K_1 , K_2 , η_1 and η_2 may all become rational indices. This is called compound twinning, and the two twin crystals have both symmetry characteristics. With respect to the transformation twins as a lattice invariant strain, the following is proved:¹⁹ K_1 for type I twinning must originate from the mirror plane in the parent phase, while η_1 for type II twinning must originate from the two-fold axis in the parent phase. The twinning elements can be calculated by the Bilby–Crocker theory,²⁰ and they are listed in Table 1.1²¹ for various MTs, which are experimentally confirmed. See Refs. [20,22,32] for the details of deformation twinning.

Table 1.1. *Twinning modes in martensite*²¹

Structure	Twinning Elements				Alloys Observed
	K_1	K_2	η_1	η_2	
BCC (FCC \rightarrow BCC) BCT	$\{112\}$	$\{\bar{1}\bar{1}2\}$	$\langle\bar{1}\bar{1}1\rangle$	$\langle111\rangle$	$1/\sqrt{2}$ Fe-Ni, Fe-Pt
(FCC \rightarrow BCT) BCT (BCC \rightarrow BCT)	$\{112\}$ $\{011\}$ $\{011\}$	$\{\bar{1}\bar{1}2\}$ $\{011\}$ $\{011\}$	$\langle\bar{1}\bar{1}1\rangle$ $\langle011\rangle$ $\langle011\rangle$	$\langle111\rangle$ $\langle011\rangle$ $\langle011\rangle$	$(2 - \gamma^2)/\sqrt{2\gamma^2}$ $\gamma - 1/\gamma$ $\gamma - 1/\gamma$ Fe-C, Fe-Ni-C, Fe-Cr-C Fe-C Au-Mn
FCT (FCC \rightarrow FCT) Tetragonal (B2 \rightarrow 3R)	$\{011\}$ $\{111\}$	$\{01\bar{1}\}$ $\{11\bar{1}\}$	$\langle01\bar{1}\rangle$ $\langle11\bar{2}\rangle$	$\langle011\rangle$ $\langle112\rangle$	$\gamma - 1/\gamma$ $\sqrt{2\gamma - 1/\sqrt{2\gamma}}$ In-Tl, Mn-Cu, In-Cd In-Pb, Fe-Pt, Fe-Pd Ni-Al
HCP (BCC \rightarrow HCP)	$\{10\bar{1}1\}$	irrational	irrational	$\{4153\}$	$\frac{\sqrt{4\gamma^4 - 17\gamma^2 + 27}}{2\sqrt{3\gamma}}$ Ti, Ti-Mo, Ti-V
Orthorhombic 2H (DO ₃ \rightarrow 2H)	$\{121\}$ $\{\bar{1}, 1.5036, 0.5036\}$ $\{101\}$ $\{111\}$	$\{\bar{1}, 1.5036, 0.5036\}$ $\{121\}$ $\{101\}$ $\{1, 0.7073, 1.2927\}$	$\langle\bar{1}, 0.7953, 0.5907\rangle$ $\langle111\rangle$ $\langle101\rangle$ $\langle1, 0.3740, 0.6260\rangle$	$\langle111\rangle$ $\langle\bar{1}, 0.7953, 0.5907\rangle$ $\langle101\rangle$ $\langle211\rangle$	0.261 ^b 0.261 ^b 0.0744 ^b 0.156 ^c Cu-Al-Ni, Cu-Al, Cu-Sn Cu-Al-Ni Cu-Al-Ni Au-Cd, Ag-Cd, Ti-Ta
2H (B2 \rightarrow 2H) Orthorhombic (BCC \rightarrow Orthorhombic)	$\{\bar{1}11\}$ $\{0.522, 0.823, 0.221\}$	$\{0.522, 0.823, 0.221\}$ $\{\bar{1}11\}$	$\langle0.788, 0.579, 0.209\rangle$ $\langle211\rangle$	$\langle\bar{2}11\rangle$ $\langle0.788, 0.579, 0.209\rangle$	0.19 ^d 0.19 ^d Ti-Ta
Monoclinic (B2 \rightarrow Monoclinic)	$\{\bar{1}11\}$ $\{111\}$ $\{0.7205, 1, 1\}$ (001)	$\{0.2470, 0.5061, 1\}$ $\{0.6688, 0.3375, 1\}$ $\{011\}$ (100)	$\langle0.5404, 0.4596, 1\rangle$ $\langle1.5117, 0.5117, 1\rangle$ $\langle011\rangle$ [100]	$\langle\bar{2}11\rangle$ $\langle211\rangle$ $\langle1.5727, 1, 1\rangle$ [001]	0.310 ^e 0.142 ^f 0.280 ^g 0.238 Ti-Ni Ti-Ni Ti-Ni Ti-Ni

In the above table, irrational numbers depend upon the values of lattice parameters. Thus these values are shown for specific alloys indicated.

^a $\gamma = c/a$ ^b Cu-Al-Ni [47] ^c Au-Cd ^d Ti-Ta [48] ^e Ti-Ni [49] ^f Ti-Ni [50]

1.2.4 Essence of the phenomenological theory of martensitic transformations

The final target of the theory of martensitic transformations from a crystallographic point of view is to predict quantitatively all the crystallographic parameters associated with the transformations, such as habit plane and orientation relationship between parent and martensite etc. We now have two theories, the so-called ‘phenomenological theories of martensitic transformations’, which make the predictions possible. These were developed by Wechsler–Lieberman–Read (WLR)^{24,25} and Bowles–Mackenzie (BM)²⁶ independently. Although the formulations are different, they are shown to be equivalent.²⁷ Since it is difficult to explain the theory in this short section, we describe only the basic ideas of the theory in order to understand the later sections, following the WLR theory, which is easier to follow physically.

The shape strain matrix \mathbf{P}_1 as an operator, representing the whole MT is given as follows.

$$\mathbf{P}_1 = \Phi_1 \mathbf{P}_2 \mathbf{B}, \quad (1.14)$$

where \mathbf{B} represents the lattice deformation matrix to create a martensite lattice from a parent lattice, \mathbf{P}_2 a lattice invariant shear matrix, and Φ_1 a lattice rotation matrix. In the theory, we focus attention on minimizing the strain energy associated with the transformation. Since such strains concentrate at the boundary between parent and martensite, we can eliminate such strains effectively by making the boundary an invariant plane, which is undistorted and unrotated on average. Since the invariant plane cannot be made only by \mathbf{B} , \mathbf{P}_2 is necessary, as schematically shown in Fig. 1.7. Although an undistorted plane can be made by the introduction of \mathbf{P}_2 , another Φ_1 is necessary to make it unrotated. Thus, \mathbf{P}_1 is given by Eq. (1.14). That is, solving Eq. (1.14) under an invariant plane strain condition is the essence of the ‘phenomenological theory’, and the habit plane is given by the invariant plane. Although we omit the detailed descriptions, we continue to explain the basic ideas in the following. If we write $\mathbf{P}_2 \mathbf{B} = \mathbf{F}$, it is always possible to separate \mathbf{F} into the product of a symmetric matrix \mathbf{F}_s and a rotation matrix Ψ , and the symmetric matrix can be diagonalized by the principal axis transformation. Thus,

$$\mathbf{F} = \Psi \mathbf{F}_s = \Psi \mathbf{\Gamma} \mathbf{F}_d \mathbf{\Gamma}^T, \quad (1.15)$$

where \mathbf{F}_d is a diagonal matrix, $\mathbf{\Gamma}$ is a matrix for the diagonalization, and $\mathbf{\Gamma}^T$ is a transpose of $\mathbf{\Gamma}$. By inserting this into Eq. (1.14), we obtain,